# Measurement of surface topography of magnetic tapes by Mirau interferometry

**Bharat Bhushan, James C. Wyant, and Chris Koliopoulos**

**Stylus-profiling techniques cannot be used for surface characterization of polymeric surfaces, such as magnetic tapes, because of their relatively low hardness An interferometric-optical-profiling microscope system was used to obtain high-accuracy surface profiles of magnetic media, rapidly and without physical contact with the sample. The profilometer consists of a conventional, reflection-type optical microscope with a Mirau two-beam interferometer attachment. The interference patterns of the surface can be observed through the eyepieces and can be detected with a solid-state linear array of 1024 detector elements. By translating the reference surface of the interferometer with a piezoelectric transducer while taking consecutive measurements, accurate surface-height measurements can be obtained from each detector element. The microscope system is controlled by a microcomputer, which communicates with a desk-top computer for further analysis of the surface-profile data. A computer-controlled specimen stage is added to increase the sample size. The reasons for selecting the Mirau two-beam interferometry are also discussed. Sample data of magnetic tapes are presented. Experimental data presented in the paper show that optimization of surface roughness is necessary to obtain optimum magnetic amplitude. friction, and wear properties.**

## I. Introduction

It is well known that surfaces are rough on a microscopic scale. When two surfaces come in contact, the contact takes place at the tip of the asperities. The load-bearing area is the real area of contact and is generally very small compared with the apparent area. The real area of contact affects the friction and wear during the sliding of the two surfaces The major thrust in this field has been on defining and measuring surface-topography parameters that affect surface interaction.[1-4]

Understanding the surface topography of magnetic head-to-tape interfaces is of great interest in conventional magnetic recording. Most asperity contacts in a head-polymeric medium are elastic; therefore, the real area of contact and friction depends on surface topography.[5] A rougher tape surface leads to lower friction. Because the linear bit density and the resolution of recorded signals increase with decreased head-to-tape spacing, close proximity between the read/write head and the tape is essential. This generally results in occasional contact at the high asperities and, consequently, in higher wear. For magnetics and wear considerations, a smoother tape surface is desirable. Hence, complete surface characterization of the magnetic medium is essential for optimization of magnetic and tribological properties The importance of surface characterization cannot be overemphasized.

In this paper, a survey of surface-roughness measurement techniques is presented, and one of them was selected for tape-surface measurements. The influence of surface roughness on magnetic-tape performance is discussed.

## II. Surface-Roughness Measurement Survey

A commonly used tool to measure surface topography is a stylus instrument such as the Talysurf or Talystep.[6] The stylus instruments are quite adequate for hard, smooth surfaces, offering excellent accuracy <l nm and lateral resolution of <l μm. However, in the case of polymers (magnetic media), the stylus digs into the surface (Fig. 1) and the results do not truly represent the microtopography. Other possible criticisms of stylus instruments for surface profiling include their sensitivity to microphonics and vibrations, particularly during long (tens of seconds) measurement times, uncertainty in point of contact of stylus on rough surfaces, and the delicate nature of their stylus and mechanism. For many years, therefore, attempts have been made to develop alternatives to the stylus instrument for surface measurement[7] including pneumatic, capacitive, thermal, resistive, frictional, and many others.

**Bharat Bhushan is with IRM Corporation, General Products Division. Tucson, Arizona 85744: the other authors are with University of Arizona. Optical Sciences Center, Tucson. Arizona 85721.**

**Received 23 Novemher 1984.**

**0003-6935/85/101489-OO$O2.00/0.**

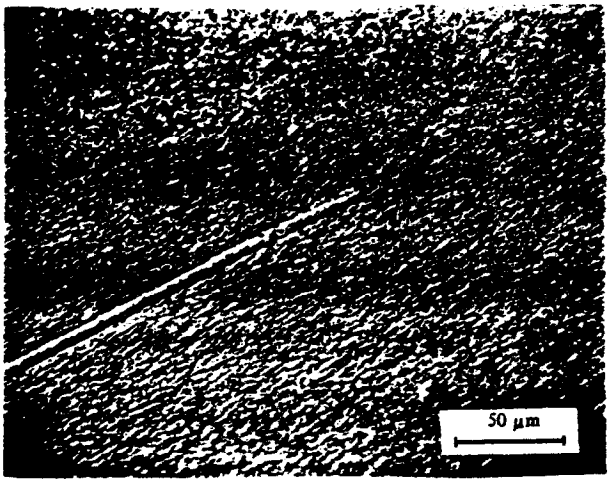


**Fig. 1. Optical micrograph of a trace made by a Talysurf 10 stylus on a typical computer tape (stylus material, diamond; stylus tip width = 25 μm; stylus load = 100 mg).**

A noncontact measurement instrument is much preferred to a contact-type instrument for surface characterization of magnetic tapes. Several noncontact techniques have been investigated for the measurement of surface roughness. These include scanning electron microscopes (SEM), light scattering approaches, light sectioning, and various interferometric techniques, such as fringes of equal chromatic order (FECO), Nomarski, and differential interference contrast (DIG), Tolansky multiple-beam interferometry, and two-beam interferometry based on Michelson, Linnik, and Mirau.

Sato and O-Hori[8] derived the profile of the surface roughness by integrating the intensity of backscattered electronic signals. Disadvantages of this technique are (1) it requires the use of a SEM, which is very expensive and not portable; (2) the sample to be measured must have a conductive coating; and (3) the total time required to perform the test is longer than desired.

Light-scattering methods represent simple and straightforward implementations, yet do not measure surface structure directly. The simplest instrument of this type is the glossmeter (ISO 2812 or ASTM D523), which measures the specular reflectance of the surface, with a variation being to measure the reflectance at some fixed angle.[9] Specular reflectance, however, increases with an increase in the refractive index and is also influenced by the smoothness of the test surface. Therefore, gloss data are not a sole function of surface topography; at best it gives an average surface topography.

Clarke and Thomas[10] have developed a laser scanning analyzer system, where a laser beam is reflected from a polygonal mirror rotating at high speed down onto a workpiece surface. It is then reflected into a fixed photoconductor receiver with a wide aperture, used to measure defects and a narrow slit for the measurement of surface roughness. With a minimum spot size on the surface of 200 μm, this approach measures the angular reflectance or scattering from the test surface over an angular range of ± 30°. Unfortunately, this scanning approach measures a specific angular reflectance at different locations on the surface and thus represents only an average angular reflectance of the test surface over the scanning range. It is from this that rms roughness and slope information are deduced.

Differential light-scattering techniques (e.g., Stover,[11] Church,[12] etc.) involve the quantitative measurement of the intensity of the scattered light as a function of scattering angle. To obtain quantitative surface parameters, certain assumptions to diffraction theory are made. The rms roughness must be small compared to the wavelength, and the height distribution of the surface microirregularities is usually assumed to be Gaussian. To obtain a spectral-density function, the surface is decomposed to sinusoidal gratings of varying amplitude and spatial frequency.

These techniques inherently average over a region of the test surface and cannot directly obtain surface profiles. The accurate measurement of scattered light over many orders of magnitude from the specular direction to nearly 90° from the specular direction is quite difficult and time-consuming. Surface preparation is important (cleanliness) for measurements of very smooth surfaces. For very rough surfaces, vector-diffraction theory must be used to predict surface structure.

Optical interferometric techniques are believed to be most promising for noncontact surface measurement since they give a direct measure of surface height. With suitable computer analysis, these can be used to completely characterize a surface. Bennett[13] has developed an interferometric system employing multiple-beam fringes of equal chromatic order (FECO). FECO are formed when a collimated beam of white light undergoes multiple reflections between two partially silvered surfaces, one of which is the surface whose profile is being measured and the other is a supersmooth reference surface. Based on a TV camera for the detection of the positional displacement of the fringes, this technique has yielded accuracies of the order of 0.80-nm rms for the measurement of surface profiles. Lateral resolution of this system has been reported to be between 2 and 4 μm over a l-mm profile length. Signal averaging in this system increases measurement time and therefore fairly severe environmental precautions must be taken to ensure measurement accuracy. Also, the system requires that the surface being analyzed have high reflectivity.

Both the DIC and the Nomarksi polarization interferometer techniques[14,15] are useful for qualitative assessments of surface topography, however, quantitative results may be difficult to obtain. While these interferometers are very easy to operate, and they are essentially insensitive to vibration, they have the disadvantage that they measure what is essentially the slope of the surface errors rather than the surface errors themselves. Furthermore, since they measure surface slope errors in only one direction, sample orientation is important.

The Tolansky or multiple-beam interferometer is

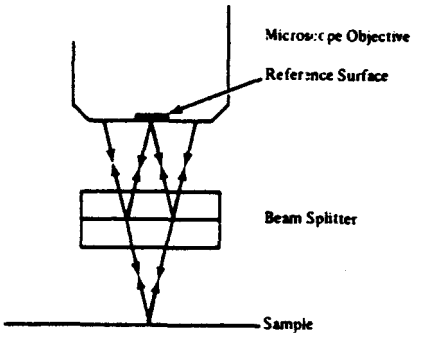


**Fig. 2. Mirau interferometer.**

another common interferometer used with a microscope. The surface being examined must have a high reflectivity and must be in near contact with the interferometer reference surface, which can scratch the surface under test.

Probably the best optical method for the measurement of surface roughness is to use a two-beam interferometer. The actual sample can be measured directly without applying a high-reflectivity coating. Since the surface-height profile itself is being measured, the actual values of the heights, slopes, and curvatures of asperities can be determined. The option of changing the magnification can be used to obtain different values of lateral resolution and different fields of view. Using electronic phase measurements, to be described subsequently, surface heights can be measured to a precision of <1 nm.

While several two-beam interferometers can be used to measure surface roughness, the Mirau interferometer's" was selected for the instrument used in this research.[18,19] A schematic of the Mirau interferometer is illustrated in Fig. 2. The interferometer is an attachment to a long working-distance microscope objective. Light from the microscope illuminator is incident on the microscope objective. Part of the light goes to the sample under test and the rest of the light is reflected by the beam splitter to the reference surface. The light reflected by the sample and the light reflected by the reference surface are combined again at the beam splitter. These two light beams interfere. The resulting interference fringes give the difference between the sample surface and the reference surface.

A major advantage of the Mirau interferometer compared with other two-beam interferometers (for example, the Linnik) is that the interferometer is common-path up to the beam splitter plate. Because the two beams of the interferometer are created after the microscope objective, the same aberrations caused by the microscope objective (and all optics before the beam splitter) are present in both arms and yield no net optical path difference when the two beams are combined for interference. Small perturbations in the optical path caused by the beam splitter plate are averaged, because the interference in the Mirau interferometer is localized at the test and reference surfaces. The Leitz Mirau interferometer used in this system has three reference surfaces on the reference plate that can be rotated into position, each with a different reflectivity, allowing the optimization of interference fringe contrast for test surfaces of different reflectivity. Each reference surface is only a few millimeters in diameter.

The Mirau interferometer does have the disadvantage that it requires a long working-distance microscope objective to accommodate the two plates, which consist of the reference surface and the beam splitter plate. This limits the numerical aperture to 0.6. The reference surface modifies the optical transfer function of the objective because the reference surface is a central obscuration in the beam. This has the effect of reducing the contrast somewhat for larger field-of-view optical systems.

A Mirau optical profilometer is developed and discussed below.

## III. Mirau Optical Profilometer

### A. Electronic Phase Measurement

Several electric phase-measurement techniques can be used in an optical profilometer[20-23] to give much more accurate height-measurement capability than can be obtained simply by looking at the interference fringes and measuring how they depart from being straight and equally spaced. Two techniques that work rather well with solid-state detector arrays are the phase-stepping technique and the integrating-bucket technique. The phase-stepping technique was used by Wyant et al.[19] The advantage of the integrated-bucket technique is that the reference surface is moved at a constant velocity rather than stepping it as in the phase-shifting technique, and hence the vibration introduced into the system is minimized. The integrating-bucket technique was implemented in the profilometer used in this paper and will be described subsequently.

Once the phase Ø(x) is determined across the interference field, the corresponding height distribution h(x) is determined by the equation

$$h(x) = (\lambda/4\pi)\phi(x). \tag{1}$$

In the integrating three-bucket technique, the phase of the reference beam is changed at a constant rate Ø(t), and every time the phase change is 90° the detector is read out. The basic equation for intensity of the two-beam interference, where the first term is the average intensity and the second term represents the interference term, is given by

$$I = I_1 + I_2 \cos[\phi(x) + \phi(t)]. \tag{2}$$

If the intensity is integrated while Ø(t) varies from 0 to $\pi/2$, $\pi/2$ to $\pi$, and $\pi$ to $3\pi/2$, the resulting signals are given by A(x), B(x), and C(x), as follows:

$$\left.\begin{aligned} A(x) &= I_1' + I_2' [\cos\phi(x) - \sin\phi(x)], \\ B(x) &= I_1' + I_2' [-\cos\phi(x) + \sin\phi(x)], \\ C(x) &= I_1' + I_2' [-\cos\phi(x) + \sin\phi(x)]. \end{aligned}\right\} \tag{3}$$

From the values of A, B, and C, the phase Ø(x) can be calculated as

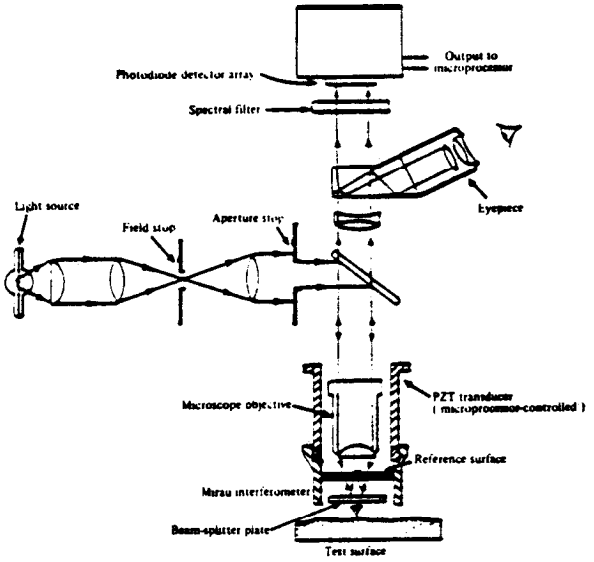


**Fig. 3. Schematic of the optical profilometer.**

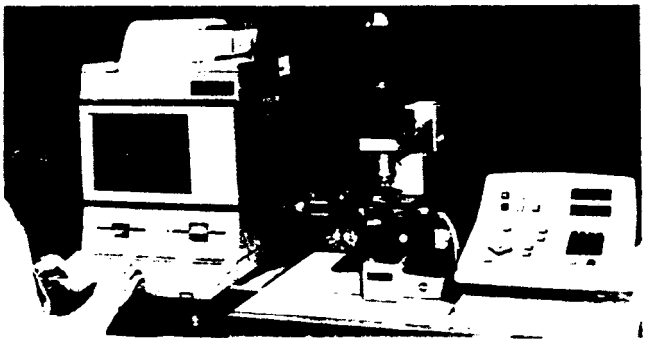

**Fig. 4. Photograph of the optical profilometer.**

$$\phi(x) = \tan^{-1}\{[C(x) - B(x)]/[A(x) - B(x)]\}. \quad (4)$$

This phase measurement is performed at each detector point. Because of the subtraction and division, the effects of fixed-pattern noise and gain variations across the detector are canceled out. as long as the effects are not so large as to make the dynamic range of the detector too small to be of use.

Figure 3 shows a schematic of the digital optical profilometer (DOP). Figure 4 shows a photograph of the instrument.

### B. interference Microscope

The profilometer uses an interference microscope (based on the principle of interferometry) modified to incorporate an optical phase-shifting device and a solid-state linear array of 1024 detectors. The number was increased from 256 (Ref. 19) to 1024 to increase the sample size. When one looks through the eyepieces interference fringes are seen. These interference fringes illuminate the linear detector array.

The electronic phase measurement technique described above is used to measure the surface height variations across the sample. The reference surface on the Mirau interferometer (objective, reference, and beam splitter plates) is attached to the piezoelectric transducer. By applying a voltage to the piezoelectric transducer, the reference surface can be translated to vary the phase of the reference beam. A microprocessor controls the voltage applied to the piezoelectric transducer in such a way that the reference surface moves at a constant rate. When the phase of the reference beam is changed 90° the linear detector array is read out and the values are stored in the memory of the microprocessor. After the array is read out three times, the microprocessor uses Eq. (4) to solve for the phase distribution across the detector array and hence the surface height variations across the portion of the sample imaged onto the detector array.

The microscope was modified to be used with 10 and 20X objectives to give a pixel spacing of 1.3 and 0.65 μm, respectively. With the linear detection array of 1024 elements (13-μm square), a total field of either 1.33 or 0.666 mm on the sample is obtained.

A lateral resolution ranges from 1.3 μm with a 10X objective to 0.65 μm with a 20X objective. A computer-controlled specimen stage is added so data can easily be taken over larger fields. The minimum and maximum step sixes of the state are 1 and 6000 μm, respectively. Stepping can be programmed to cover a rectangular area or predetermined path. Slewing rates are 10 - 6000 μm/sec.

## IV. Data Analysis

### A. Statistical Parameters of Interest

For many rough surfaces of engineering importance, surface height and gradients are random and have a Gaussian probability distribution. In this case, the probability density function is given by

$$p(x) = (1/\sigma\sqrt{2\pi}) \exp[-(x - \mu)^2/2\sigma^2], \quad (5)$$

where $\mu$ is the mean and $\sigma$ is the standard deviation of the surface height. Nayak[24] has shown that a larger number of useful statistics of the surfaces may be found for random, isotropic, Gaussian surfaces if the first three momenta of the power spectral density function, $m_0 m_2$ and $m_4$, are known.

Once a surface profile x(t) is obtained, the autocorrelation of the profile may be calculated using the following equation:

$$R(\tau) = \lim_{T \to \infty} (1/T) \int_0^T x(t)x(t + \tau)dt. \quad (6)$$

Note that $R(0) = \text{rms}^2 = \sigma^2 + \mu^2$.

The power spectral density (PSD) function is found by the Fourier transform of the autocorrelation function:

$$S(f) = \int_{-\infty}^{\infty} R(\tau) \exp(-j2\pi f\tau)d\tau. \quad (7)$$

(The autocorrelation function is the inverse Fourier transform of the PSD function.)

Moments of the power spectral density function are given by

$$m_n = (2\pi)^n \int_{-\infty}^{\infty} f^n S(f)\,df. \tag{8}$$

In very general conditions, the spectral moment $m_n$ *is* the mean-square value of the (n/2) derivative of the surface profile (Nayak[24]). Therefore, $m_0$ $m_2$, and $m_4$ are given as

$$m_0 = \sigma^2, \qquad m_2 = \sigma_\theta^2 \qquad m_4 = \sigma''^2 \tag{9}$$

where $\sigma_\theta$ and $\sigma$ " are the standard deviations of the surface slope (first derivative of surface profile) and surface curvature (second derivative of the surface profile).

Nayak has also defined the following auxiliary quantity $\alpha$:

$$\alpha = (m_0 m_4/m_2^2) = [(\sigma\sigma'')^2/\sigma_\theta^4], \tag{10}$$

which defines the width of the power spectrum of the random process forming the surface from which the profile is taken. If a $\rightarrow$ 1, the spectrum consists of a single frequency. If $\alpha \rightarrow \infty$, the spectrum extends over all frequencies. When $\alpha \rightarrow \infty$, the peak heights have a Gaussian distribution and the mean curvature is nearly constant $(= 8\sigma''/3\sqrt{\pi})$. Curvature vs peak height and probability density of peak heights for any a can be obtained using Nayak's analysis (see also Ref. 25).

If Greenwood and Williamson's' analysis is to be applied for determination of real area of contact and if junctions are elastic or plastic (for tribological considerations), the standard deviations of peak height (assumed to be of Gaussian distribution) and mean curvature (assumed to be constant) are needed. (Baaed on Nayak's analysis, their assumption is only satisfied if $\alpha \rightarrow \infty$.) The desired values can be obtained from Nayak's analysis or can be measured directly. Gupta and Cook[26] have further argued that very few peaks interact and assumed arbitrarily that upper 25% peaks are important.

Using discrete random-process analysis, Whitehouse and Phillips' have shown that, if the surface profile has a Gaussian distribution (which is true in most cases), the peak data required by Greenwood's analysis can be obtained from $\sigma$ and the value of the autocorrelation function at the first two intervals. The autocorrelation distance (for an exponential distribution, the distance where its value drops to 10% of the value at zero distance) is also important in the calculation of sample length.

Blok[27] and Halliday[28] have proposed that junctions are elastic provided the asperity slope is less than H/ $\pi$ E', where H is the hardness and E' is the reduced modulus.

The number of zero crossings $N_0$, the number of peaks per unit length $N_p$, and the peak density $N_s$ are also of interest. The ratio $N_o/N_p$ is considered to be important.. A lower value would lead toward plastic contact or lower real area of contact. However, for favorable magnetic amplitudes, No/$N_p$, should be close to 1. These parameters can either be directly measured or can be obtained from the following equations[24,25]:

$$\left.\begin{aligned} N_0 &= (1/\pi)(\sigma_\theta/\sigma), \\ N_p &= (1/2\pi)(\sigma''/\sigma_\theta), \\ N_s &\sim 1.2N_p^2. \end{aligned}\right\} \tag{11}$$

To have the complete flexibility of using any of the analyses mentioned so far, software was developed to predict all the statistical parameters stated so far: surface height, slope, and curvature; peak and upper 25% peak heights, absolute (mean asperity) slope, and curvature; number of zero crossings, number of peaks, and peak density; and autocorrelation function. Once the height distribution across the sample is measured at 1024 points, the data can be analyzed to determine many statistical properties about the magnetic tape being studied. The height distribution across the sample is fitted, in a least-squares sense, to determine the average height, the tilt across the sample, and the curvature. The average height and tilt are subtracted from the height distribution. In the analysis of tape samples, the curvature is generally subtracted before the surface profile is plotted, because the curvature is the result of the tape sample not being held flat. The peak-valley distance (P-V) is determined by subtracting the lowest height measured from the highest height measured. The root mean square (rms) of the height distribution is also calculated. For details on determining other statistical properties, see Wyant et al. [19]

## B. Resolution, Repeatability, and Accuracy

The lateral resolution of the instrument is of the order of pixel spacing. The repeatability of the instrument is of the order of 0.l-1-nm rms. The repeatability depends on how rough the surface is and how good the surface reflectivity is. A typical repeatability for the magnetic media analyzed for this study was 0.5-nm rms. This number was determined by obtaining a surface profile and storing the data in the computer, repeating the measurement of the surface profile, and then subtracting these two profiles and finding the rms of the difference.

The repeatability can be further improved by averaging the number of data sets in a single run. In a trial run, the number of data sets averaged varied from 1 to 10 and the difference in rms in two identical runs was measured and the results are reported in Table I. We note that if four data sets are averaged in each run, the repeatability error would be <0.5 nm.

Accuracy of the instrument reported in Ref. 19 is within (perhaps less than) 1 nm.

## V. Results and Discussions

The first series of tests was conducted to determine the statistical sample size for objective magnifications of 10 and 20. In each case, 16 runs were made longitudinally 500 μm apart across the width of the tape at two adjacent locations ~20 cm apart. Net rms and other parameters were calculated at each location. Typical surface profile, histogram, and distribution of surface heights on location 1 at 20X are shown in Fig. 5. Surface heights follow a Gaussian distribution. No important differences can be observed between 10 and 20x. A summary of all the results is given in Table II. We note that surface rms at 20X is slightly lower than at 10X. It is believed that a more accurate value is obtained at 20X. Surface and peak slopes and curvatures are larger at 20X than at 10X and the number of peaks is lower at 20X than at 10X, as expected.

**Table 1. Repeatability**

| No. of sets averaged | Noise rms (A) |
|---|---|
| 1 | 11.5 |
| 2 | 9.8 |
| 3 | 6.5 |
| 4 | 5.2 |
| 6 | 4.6 |
| 8 | 3.8 |
| 10 | 3.5 |

Noise rms is based on the average of three duplicate measurements.

Surface rms was calculated for each run, then net rms was calculated by adding one run at a time:

$$\sigma^2_{\text{net}} = \sum_{i=1}^{n} \sigma_i^2/n^2, \quad (12)$$

where n is the number of runs The data are plotted in Fig. 6. We find that 3-4 runs should be made at 10X and 4-6 runs at 20X. The computer-controlled specimen stage can be used to achieve multiple traces.

Whitehouse and Phillips[2] have defined a criteria for calculation of statistical sample size. According to their analysis, for a 5% standard deviation of the mean of a rms data set,

**sampling length = X 200 autocorrelation distance.**

The autocorrelation distance of tape AA is 0.019 and 0.023 mm at 10X and 20X, respectively. Center-to-center distance between the pixel elements is 1.3 μm at 20X and 0.65 μm at 20X. Therefore total length tra-

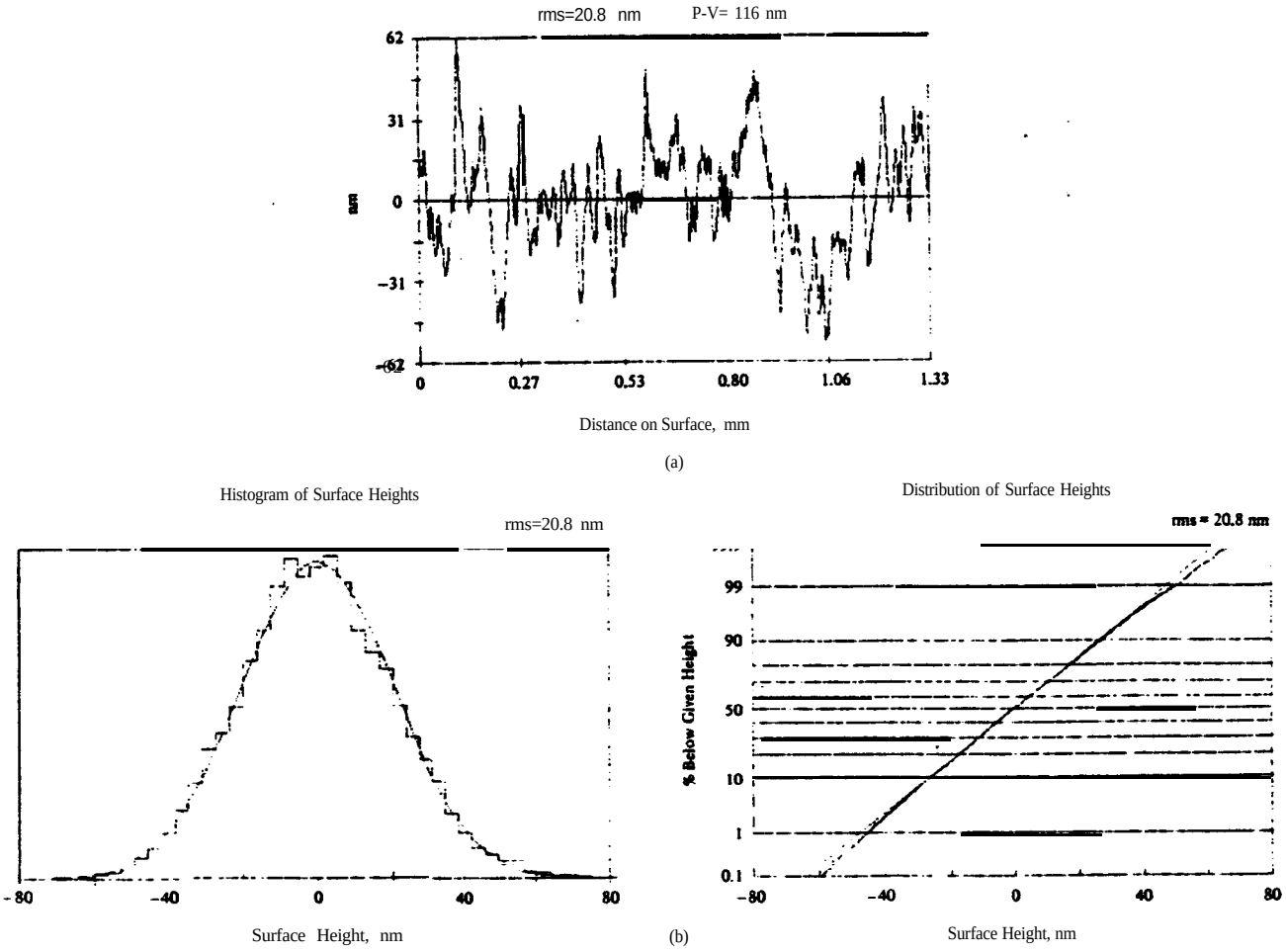


**Fig. 5. Surface profile of a magnetic tape AA at an objective magnification of 20X. (b) Histogram and distribution of surface heights.**

**Fig. 6. Variations of rms with nunber of data sets for tape AA at objective magnifications of (a) 20X and (b) 10x.**

**Table II. Measured Surface Topography Parameters for Tape *AA* at Objective Magnifications of 10X and 20X (Location 1, Fig. 6)[a,b]**

| Objective mag. | rms surface height nm | rms surface slope $\times 10^{-3}$ | rms surface curvature 1/mm | Peaks/upper 25% peaks Height Mean nm | Height $\sigma$ nm | Slope Mean $\times 10^{-3}$ | Slope $\sigma$ $\times 10^{-3}$ | Curvature Mean 1/mm | Curvature $\sigma$ 1/mm | Peak-to-valley distance nm | Number of P/UP[b] /mm | No.[c] 1/mm | ACD[d] 1/mm |
|---|---|---|---|---|---|---|---|---|---|---|---|---|---|
| 10X | 18.8 | 2.9 | 2.15 | 5.8/30.5 | 19.2/10.3 | 0.93/1.13 | 0.90/0.93 | 3.18/3.45 | 1.35/1.48 | 141.3 | 224/138 | 124 | 0.028 |
| 20X | 20.5 | 5.4 | 7.37 | 6.0/32.2 | 20.3/10.9 | 1.7/2.1 | 1.9/2.1 | 11.53/12.53 | 5.16/6.30 | 145.0 | 169/103 | 104 | 0.024 |

[a] The data reported here are based on 16 runs 500 $\mu$m apart across the width of the tape.
[b] P/UP, all peaks/peaks above mean.
[c] No. number of zero crossings per mm.
[d] ACD, autocorrelation distance at which autocorrelation function drops to 0.1 of its original value.

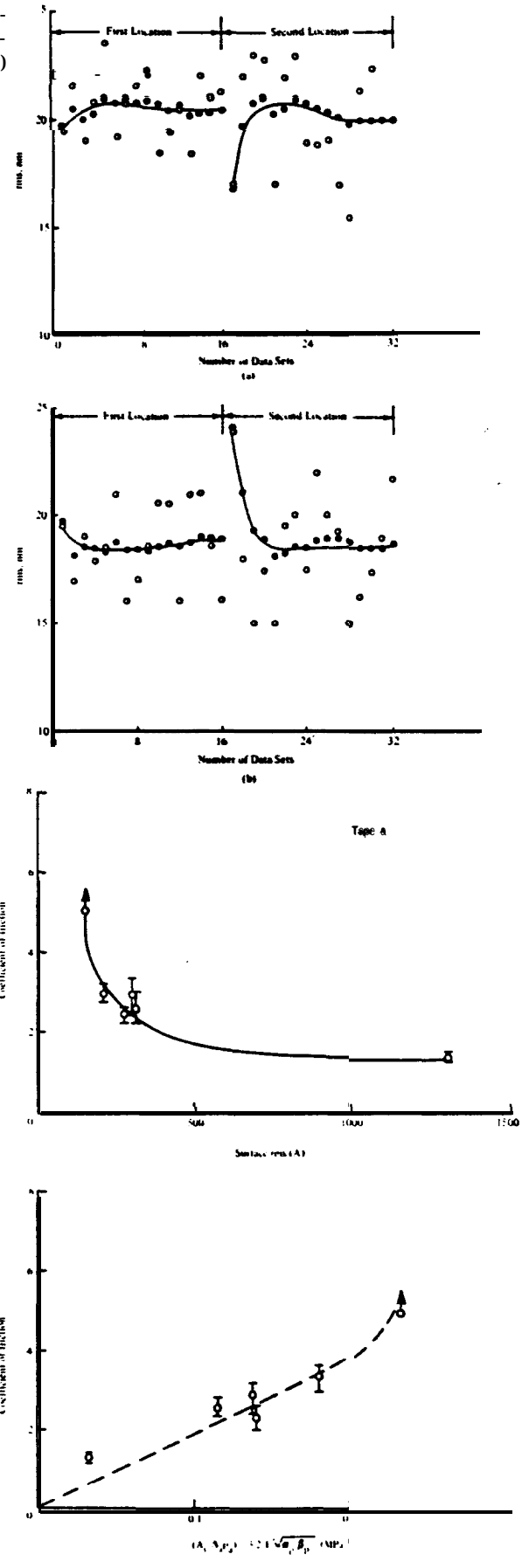


**Fig. 7.** Influence of surface roughness on the coefficient of friction.

versed at 10 and 20x is 1.33 and 0.67 mm, respectively. Sampling length and number of data sets required are given in Table III.

We therefore note that our prediction of number of data sets is consistent with that predicted by the analysis of Whitehouse and Phillips.[2] Since the results at 20X are believed to be more accurate than at 10X, we recommend use of the 20X objective unless autocorrelation distance of the test surface is very large requiring a large number of runs.

The sample data of commercial tapes are given in Table IV. From distributions and the value of $\alpha$ (reported in Table I), we note that the tape surfaces follow a Gaussian distribution. Surfaces are smooth; the mean asperity slope is of the order of 0.1°.

Experiments were conducted to study the influence of surface roughness on friction, wear, and magnetic-signal amplitude. Figure 7 shows the relationship of the coefficient of .friction vs surface rms and real area of

**Table III. Sampling Length at Different Objective Magnifications**

| Objective magnification | Pixel spacing ($\mu$m) | Length traversed (mm) | Auto correlation distance (mm) | Sampling length (mm) | No. of data sets |
|---|---|---|---|---|---|
| 10× | 1.3 | 1.3312 | 0.019 | 3.8 | 3 |
| 20× | 0.65 | 0.6656 | 0.023 | 4.6 | 7 |

Table IV. Measured Values of Typical Magnetic-Tape Surfaces

| Tape surface | rms surface height nm | rms surface slope x $10^{-3}$ | rms surface curvature l/mm | Peaks/upper 25% peaks Height σ nm | Peaks/upper 25% peaks Slope Mean x $10^{-3}$ | Peaks/upper 25% peaks Slope σ x $10^{-3}$ | Curvature Mean l/mm | Curvature σ l/mm | Peak-to-valley distance nm | P/UP[a] density /mm$^2$ | Number of P/UP /mm | No.[b] l/mm | A | C | D[c] mm | a |
|---|---|---|---|---|---|---|---|---|---|---|---|---|---|---|---|---|
| A | 26.1 | 4.0 | 1.79 | 25.6/14.3 | 2.0/2.1 | 1.3/1.1 | 2.65/2.91 | 1.54/1.69 | 123 | 6571/2788 | 74/48 | 47 | | | 0.012 | 8.52 |
| B | 31.7 | 4.9 | 2.15 | 29.8/16.7 | 2.6/3.2 | 1.6/1.4 | 2.74/3.02 | 1.44/1.54 | 161 | 5227/2430 | 66/45 | 49 | | | 0.013 | 8.06 |
| C | 31.4 | 5.3 | 2.40 | 30.2/17.3 | 2.8/3.9 | 1.9/1.9 | 2.92/3.06 | 1.56/1.61 | 177 | 5008/2281 | 65/44 | 49 | | | 0.015 | 7.20 |
| D | 21.9 | 3.5 | 1.86 | 20.9/10.9 | 1.8/2.2 | 1.2/1.2 | 2.30/2.43 | 1.31/1.30 | 118 | 6931/3146 | 76/51 | 50 | | | 0.035 | 11.06 |
| E | 20.6 | 4.2 | 2.36 | 19.9/10.1 | 2.1/2.5 | 1.5/1.4 | 2.48/2.43 | 1.57/1.37 | 143 | 7603/3448 | 80/54 | 64 | | | 0.022 | 7.60 |

[a] P/UP, all peaks/peaks above mean.
[b] No., number of zero crossings per mm.
[c] ACD, autocorrelation distance at which autocorrelation function drops to zero.

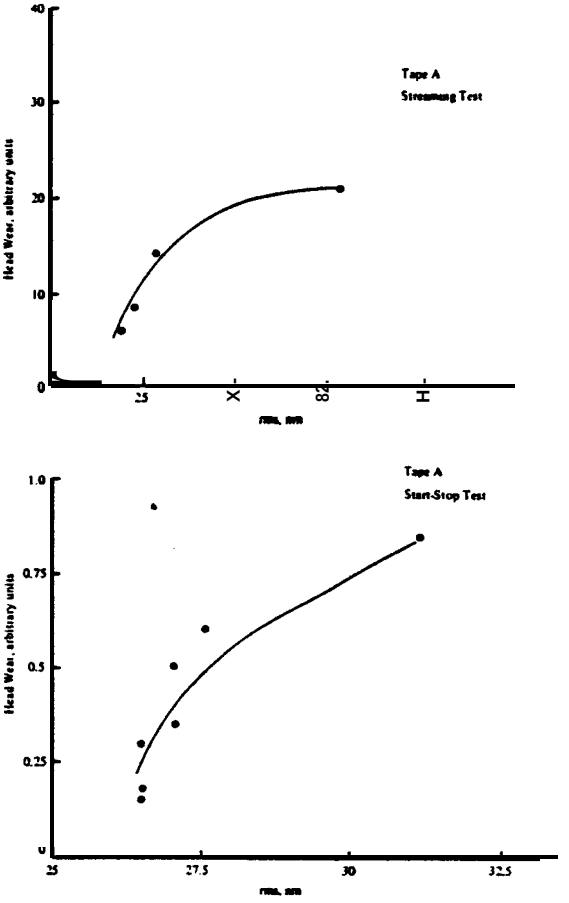


Fig. 8. Influence of surface roughness on head wear.

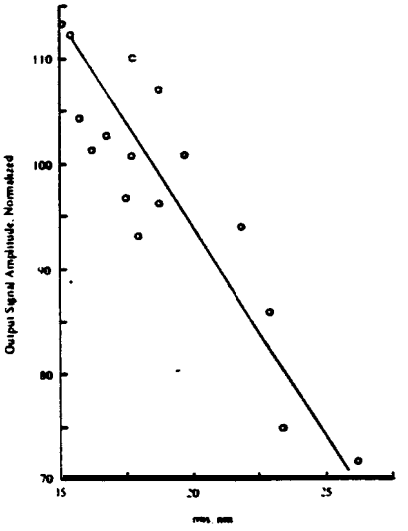


Fig. 9. Effect of surface roughness on signal amplitude. Measurements were made at 1600 flux reversals/mm.

Table V. Signal Amplitude and Surface Topography Data for a Magnetic Tape

| Parameter | Tape number A1 | A2 | A3 |
|---|---|---|---|
| Amplitude mean, %[a] | 100 | 89 | 71 |
| Standard mean at | | | |
| 0.4 kfc/mm[b] | 0.0389 | 0.0369 | 0.0454 |
| 0.8 kfc/mm | 0.0474 | 0.0499 | 0.0606 |
| 1.2 kfc/mm | 0.0542 | 0.0536 | 0.0705 |
| Surface roughness | | | |
| Standard dev., nm | 15.5 | *23.3* | *27.7* |
| Gloss no. | 120 | 166 | 80 |

[a] Output signal amplitude normalized.
[b] kfc/mm, 1000 flux changes per millimeter

contact $(A_r \alpha 1/\sqrt{\sigma_p/\beta_p},$ where $\sigma_p$ and $\beta_p$ are the standard deviation and mean radii of curvature of asperity peaks). We clearly see the importance of the surface roughness and note that there is no gain after a particular value of the surface roughness (50 nm) because junctions probably become plastic and the real area of contact no longer depends on the surface roughness[5]

Head-wear results as a function of surface roughness are reported in Fig. 8. We note that wear, both in streaming and start-stop tests, increases with surface roughness. Magnetic-signal amplitude results, presented in Table V, and additional results in Fig. 9, show that the increase in roughness results in a decrease in signal amplitude. Therefore, from both wear and magnetic-signal amplitude considerations, the smoother the surface, the better it is. However, from a friction point of view, the rougher the surface, the better it is. This clearly demonstrates the need for optimization of surface roughness.

## VI. Conclusions

A profilometer using the principle of Mirau interferometry, which provides complete surface characterization, was used for measurement of surface roughness of the magnetic tapes. Surface-topography statistics given by the system are surface height, slope, and curvature distributions; all peaks and upper 25% peak heights, absolute slopes, and curvatures; peak density and number of zero crossings per unit Iength; and autocorrelation function. The coefficient of friction decreases with an increase in surface roughness, and the converse is true for head wear and magnetic-signal amplitude. Therefore, optimization of the surface roughness is essential during the tape develop ment.

The authors thank O. E. George for his support during the development of the optical profilometer. Wear and magnetic-signal data were taken by F. W. Hahn, M. K. Haynes, and B. I. Finkelstein. respectively.

## References

1. J. A. Greenwood and J. B. P. Williamson, "Contact of Nominally Flat Surfaces." Proc. R. Soc London Ser. A 295. 300 (1966).
2. D. J. Whitehouse and M. J. Phillips, "Discrete Properties of Random Surfaces," Proc. R. Soc. London Ser. A 299, 267 (1978); 'Two-Dimensional Discrete Properties of Random Surfaces," Proc. R. Soc. London Ser A 316, 97 (1970).
3. J. B. P. Williamson, '"Topography of Solid Surfaces," in *Proceedings, NASA Symposium on Interdisciplinary Approach to Friction* and Wear, NASA SP-181 (1968), pp. 85-142.
4. Special Issues on "Metrology and Properties of Engineering *Surfaces,*" Wear 57, 1-384 (1979); *83,* l-409 (1982).
5. B. Bhushan. R. L. Bradshaw, and B. S. Sharma, "Friction in Magnetic Tapes II. Role of PhysicaI Properties," ASLE Trans. 27, 89 (1984).
6. J. M. Bennett and J. H. Dancy, "Stylus Profiling Instrument for Measuring Statistical Properties of Smooth Optical Surfaces," Appl. Opt. 20, 1785 (1981).
7. T. R Thomas, "Surface Roughness Measurement: Alternatives *to the Stylus." in Proceedings, Nineteenth International MTDR Conference* (Macmillan, London, 1979). pp. 383-396.
8. H. Sato, and M. O-Hori, "Surface Roughness Measurement by Scanning Electron Microscope," Ann. CIRP 31, 457 (1982).
9. *H. A. Gardner* and *G. G. Sward. Paint Testing Manual, Physical and Chemical Examination: points, Varnishes, Lacquers and* Colors (Gardner Laboratories Inc., Bethesda. Md.).
10. G. M. Clarke and T. R. Thomas, "Roughness Measurement with a Laser Scanning Analyzer," Wear 57, 107 (1979).
11. J. C. Stover, "Roughness Characterization of Smooth Machined Surfaces by Light Scattering," Appl. Opt. 14, 1796 (1975).
12. E. L. Church, 'The Measurement of Surface Texture and Topography by Differential Light Scattering," Wear 57, 93 (1979).
13. J. M. Bennett, "Measurement of the rms Roughness, Autocovariance Function and Other StatisticaI Properties of OpticaI Surfaces Using a FECO Scanning Interferometer," Appl. Opt. Hi.2705 (1976).
14. F. Francon, *Optical Interferometry* (Academic. New York, 1966).
15. F. Francon and S. Mallick, Polarization Interferometers (Wiley-Interscience, New York, 1971).
16. *S.* ToIansky. *Introduction to Interferometers* (Wiley, New York, 1973). pp. 213 and 214.
17. *A.* J. HaIe. *The Interference Microscope (E.* & *S.* Livingstone. London, 1958), p. 15.
18. C. L. KoliopouIos. "Interferometric OpticaI Phase Measurement Techniques," Ph.D. Dissertation, U. Arizona (1981).
19. J. C. Wyant. C. L. Koliopoulos, B. Bhushan, and O. E George, "An Optical Profilometer for Surface Characterization of Magnetic Media," ASLE Trans. 27, 101 (1984).
20. J. H. Bruning, "Fringe Scanning Interferometers," in *Optical Shop Testing,* D. Malacara. Ed. (Wiley. New York, 1978). pp. *409-437.*
21. G. E. Sommargren. "Optical Heterodyne Profilometry," Appl. Opt. 20, 610 (1981).
22. J. C. Wyant and C. L. Koliopoulos, "Phase Measurement System for Adaptive Optics," AGARD Conf. Proc. 366, 48.1 (1981).
23. J. C. Wyant, "Use of an ac Heterodyne Lateral Shear Interferometer with ReaI-Time Wavefront Corrections Systems," Appl. Opt. 14, 2622 (1975).
24. P. R. Nayak, Random Process Model of Rough Surfaces," J. Lubr. Technol. 93, 398 (1971).
25. T. E. Tallin, "The Theory of Partial Elastohydrodynamic Contacts," Wear 21, 49 (1972).
26. P. K. Gupta and N. H. Cook. "StatisticaI Analysis of Mechanical Interaction of Rough Surfaces," J. Lubr. Technol. 94F, 19 (1972).
27. H. Blok. "Comments on the Paper by R. Wilson," Proc. R. Soc. London Ser. A 212, 486 (1952).
28. J. S. Halliday, "Surface Examination of Reflection Electron Microscopy." Proc. Inst. Mech. Eng. London 109, 777 (1955).